2018 XIII International Conference on Electrical Machines (ICEM)

DOI: 10.1109/ICELMACH.2018.8507020

3D Electromagnetic and Thermal Analysis for an Optimized Wound Rotor Synchronous Machine

Huong Thao Le Luong

Frederic Messine

Carole Hénaux

Guilherme Bueno Mariani

Nicolas Voyer

Stefan Mollov

3D Electromagnetic and Thermal Analysis for an Optimized Wound Rotor Synchronous Machine

H. T. Le Luong, F. Messine, C. Hénaux, G. Bueno Mariani, N. Voyer, S. Mollov

***Abstract* -- This paper describes the 3D simulations of an optimized modular brushless wound rotor synchronous machine using finite element method and computational fluid dynamics method. 2D finite element tool is used in the optimization in order to compute the torque and iron losses. Furthermore, an analytical thermal equation is used in order to calculate the surface temperature of the machine; this equation is used instead of the lumped parameter circuit due to the complexity of the machine structure. Its advantage is to reduce the computational time and therefore, to explore more deeply the whole search domain. However, the optimal results need to be validated by more precise numerical methods. These numerical verifications show that the leakage flux in the end-winding is high, leading to high iron losses in this machine. Moreover, the surface temperature differences between the analytical and numerical methods are discussed.**

***Index Terms*—Wound rotor synchronous machine, modular machine, 3D simulation, finite element analysis, thermal analysis, computational fluid dynamics.**

I. Introduction

Modular machine with integrated drive electronics has been widely investigated in a wide range of applications, particularly in the compressor of HVAC system. A modular machine constructed based on a Poki-Poki™ machine [3] is shown in Fig. 1.

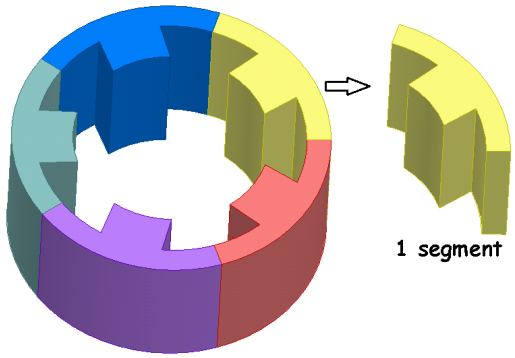

Fig. 1. An example of the segmented stator of a modular machine.

In this case, the stator core is not a massive entity. It is split into individual segments. Each segment contains one tooth and one part of the stator yoke. The coils are wound for each segment. Then, the stator is assembled into a cylindrical shape and is pressed into a frame. The advantages of these kinds of stator are the fast automatic winding manufacturing, the easiness to assemble and to remove them, and therefore, the easiness to replace a faulted component [1]-[3]. Moreover, the slot fill factor can be increased, leading to a decrease of the copper losses.

With this modular structure, each phase of the machine is connected to a separate single-phase converter. Each phase drive module is regarded as a single module and every phase can operate independently of the others. These structures are highly redundant. The effects on the other phases are minimized in case of fault in one phase and therefore, the system can continue operating even if a fault appears.

Using electromagnetic analysis, 7-phase/7-slot/6-pole wound rotor synchronous machine (WRSM) with non-overlapping fractional slot concentrated winding was selected among a set of different machines based on the criteria of torque density, efficiency and torque ripple. This machine was then compared to surface-mounted permanent magnet synchronous machine (SM-PMSM). The results demonstrated that the modular brushless WRSM presents interesting performance features including high fault tolerant capability and extended field weakening range with the performance closely matching that of an equivalent SM-PMSM, for details see [4].

With this WRSM machine, a heptagonal stator is proposed. This makes it possible to increase the slot fill factor and to provide more space to integrate the power converters on the machine frame. The 2D structure of the heptagonal WRSM is shown in Fig. 2.

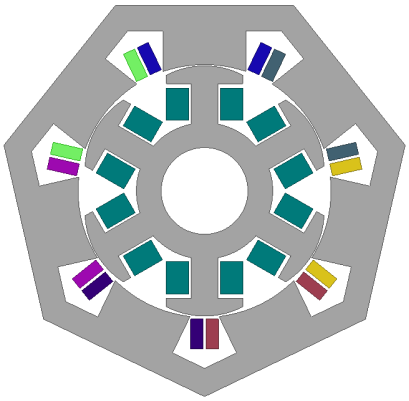

Fig. 2. 2D structure of 7-phase/7-slot/6-pole heptagonal WRSM.

In Section II, the optimized WRSM is presented and the calculation of machine temperature via an analytical equation will be explained. 3D electromagnetic validation is carried out, yielding a modification of the optimized WRSM in Section III. Section IV addresses 3D thermal

This work was supported by Mitsubishi Electric R&D Centre Europe in France through a research project with LAPLACE laboratory.

H. T. Le Luong, F. Messine, C. Hénaux are with the Laboratoire Plasma et Conversion d'Energie, University of Toulouse, Toulouse 31071, France (e-mail: hleluong@laplace.univ-tlse.fr).

H. T. Le Luong, G. Bueno Mariani, N. Voyer, and S. Mollov are with the Mitsubishi Electric R&D Centre Europe, Rennes, France.

analysis and the coil temperature will be focused on. Finally, the results are discussed in the conclusion.

II. Optimized WRSM

This machine is optimized by using a Mesh Adaptive Direct Search (MADS) based optimization algorithm. NOMAD solver is based on MADS and it is developed in Matlab Toolbox. NOMAD is well suited for optimization problems where the objective function and/or the constraints are analyzed using numerical simulations without derivative computations [5]-[7]. In this optimization problem, the objective function is to minimize the exterior volume of the machine under constraints including the average torque $= 5Nm$, the torque ripple $\leq 5\%$, the machine efficiency $\geq 94\%$ and the temperature of the coils $\leq 105°C$. Assuming that with a surface temperature of the machine $\leq 85°C$, we would be able to obtain the desired temperature of the coils.

The machine performances are analyzed thanks to ANSYS Maxwell based on the finite element method (FEM). Considering that the computational time and the complex structure of the WRSM, the surface temperature of the frame is calculated from the following equation:

$$T_s = T_{amb} + \Delta T° = T_{amb} + P_{total} \times R_\theta \qquad (1)$$

where T_s is the surface temperature of the frame, T_{amb} is the ambiance temperature, P_{total} is the total losses of the machine and R_θ is the thermal resistance for the convection which is defined as:

$$R_\theta = 1/hS \qquad (2)$$

where h is the convection heat transfer coefficient, S is the surface area of the frame.

The value of the convection heat transfer coefficient for natural convection was presented in [8]. In this study, the convection heat transfer coefficient is selected as $20\,W/m^2K$.

After optimizing, the minimal value of the exterior volume obtained is $2.0542 \times 10^6\ mm^3$. The machine performances at 7000rpm are represented in Table I and the optimized variables are shown in Table II.

TABLE I
THE PERFORMANCE OF AN OPTIMIZED WRSM

Performance	Value	Unit
Average Torque	5.00	Nm
Torque ripple	4.09%	
Stator copper loss	35.40	W
Rotor copper loss	50.74	W
Iron losses	80.13	W
Total losses	166.27	W
Efficiency	95.56%	
Temperature	86.50	°C

TABLE II
OPTIMIZED VARIABLES

Name	Value	Unit
Machine Length	31.62	mm
Stator Yoke Height	13.95	mm
Tooth Height	18.38	mm
Tooth Width	45.46	mm
Rotor Yoke Height	12.88	mm
Pole Shoe Height	9.80	mm
Pole Shoe Width	41.90	mm
Pole Body Height	22.14	mm
Pole Body Width	14.50	mm
Shaft Diameter	47.53	mm
Pole Arc Offset	23.18	mm
Armature Current Density	2.69	A/mm^2
Field Current Density	3.87	A/mm^2

Note that the optimal WRSM presented in Tables I and II are the best local optimum that we found by using NOMAD during intensive 2D-numerical efforts; from a starting point to a local solution that takes about 5 days. This is not presented in this paper which mainly deals with the 3D-numerical validations of this optimal design of WSRM.

The machine performances including the average torque, the torque ripple and the machine efficiency are then evaluated by 3D simulation taking into account the effect of the end-winding. The machine temperature will be analyzed based on computational fluid dynamics (CFD) method by using ANSYS Fluent in order to validate the optimal results.

III. 3D Electromagnetic Verification

A. Introduction

A large number of numerical methods can be considered in order to solve flux equations. FEMs have been widely used in practical applications, not only for steady-state field analysis but also for transient performance analysis of electrical machines [9]-[11].

3D-numerical models make it possible to analyze the flux in the end zone of electrical machines. Indeed, the current in the end-winding can generate leakage flux that is not included in the flux calculated from a 2D simulation. Therefore, the solution in 3D is generally more accurate than a 2D one, because it takes into account the leakage flux; the size of the 2D and 3D meshes must be comparable.

Standard non-grain-oriented electrical steel for both the stator and the rotor is M330-35A. This lamination has a good magnetic characteristic such as high permeability and low loss density. The stacking factor of the lamination is 0.95. The 3D structure of the optimal WRSM is presented in Fig. 3.

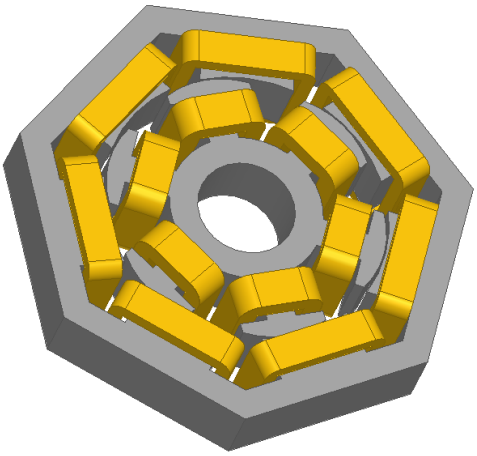

Fig. 3. 3D configuration of the optimal heptagonal WRSM.

The principle steps for modeling electric machines in ANSYS Maxwell were presented in [9]. In this study, the rotor winding is excited with DC current and the stator windings are fed by sinusoidal currents. The initial rotor position is determined in order to obtain the maximum static torque of the machine.

B. Analysis Results

It takes a lot of CPU-time and memory to simulate and analyze the performance of the optimal WRSM in 3D; this is due to the complicated shape of the windings, and a large number of mesh elements. It takes at least 60 hours to simulate the 3D model of the machine with a sufficiently thin mesh size to obtain precise results, which can be compared to 2D model of the machine (values presented in Table I). The magnetic induction of the machine is shown in Fig. 4.

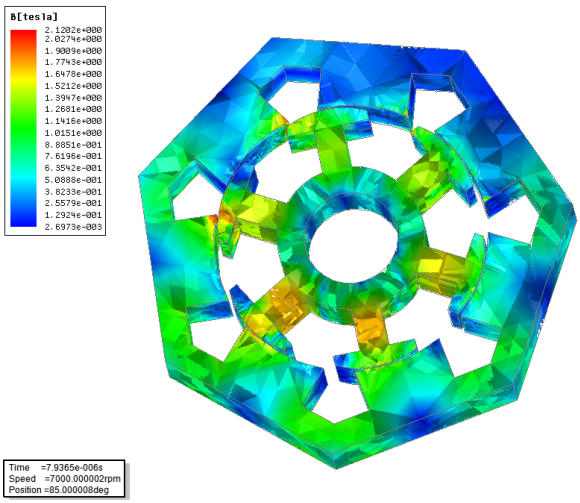

Fig. 4. Magnetic induction distribution of the stator and the rotor.

In Table III, the machine performances by using 3D FEA are provided. The average value of the torque is 4.8434Nm and the torque ripple is about 4.28%. The iron losses are higher than the value in 2D due to the leakage flux induced by the current in the end-winding. The electromagnetic efficiency of the machine is reduced to 94.79% and therefore, the surface temperature of the machine is increased to 95.75°C.

TABLE III
MACHINE PERFORMANCE USING 3D FEA

Performance	Value	Unit
Average torque	4.84	Nm
Torque ripple	4.28%	
Phase voltage (rms)	91.74	V
Stator copper loss	35.40	W
Rotor copper loss	50.74	W
Iron losses	105.14	W
Total losses	191.28	W
Efficiency	94.79%	
Temperature	95.75	°C

Note that the average torque is smaller than 5Nm. Thus, it is necessary to increase the average torque in order to obtain the desired performance. The machine length is selected to increase the average torque without affecting too much the surface temperature based on a sensibility analysis. Thanks to an analytical approximation, the new value of the machine length calculated is 32.65mm in order to obtain 5Nm for the average torque. In order to verify the results, a new 3D simulation based on FEM is carried out. The electromagnetic torque is shown in Fig. 5 and the performances of the new machine are shown in Table IV.

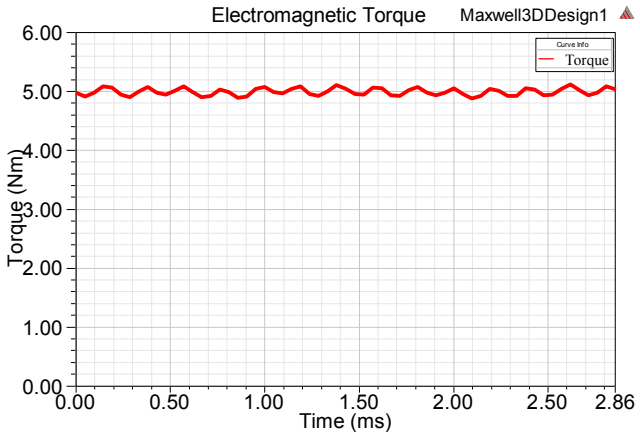

Fig. 5. Output torque of the WRSM obtained by 3D FEA.

TABLE IV
MACHINE PERFORMANCES RECTIFIED

Performance	Value	Unit
Average torque	5	Nm
Torque ripple	4.05%	
Phase voltage (rms)	94.27	V
Stator copper loss	35.80	W
Rotor copper loss	51.51	W
Iron losses	105.94	W
Total losses	193.25	W
Efficiency	94.89%	
Temperature	96.07	°C

The value of the surface temperature obtained is 9.57°C higher than the one for the optimized WSRM; this is due to

the difference of the losses. Since the main goal is to obtain less than 105°C for the coil temperature, the study shall proceed in order to evaluate the real value of the temperature of the coils in the thermal analysis.

IV. Thermal Analysis

A. Introduction

The integration of power converters onto the machine housing can raise the machine temperature. If the temperature is too high that may cause problems such as failure of insulation materials and therefore, this can decrease the lifetime of the converters and of the machine. In this study, the temperature limit is fixed to 105°C. Hence, it is necessary to determine the temperature distribution of the new corrected machine. The temperature can be achieved according to two approaches: lumped-parameter thermal method or numerical methods such as FEM and CFD.

The lumped-parameter thermal models make it possible to estimate key temperatures inside an electrical machine much more rapidly than the numerical methods. However, the calculation of the lumped parameters which are mainly based on the dimensional data of the machine can be challenging to perform for complex parts including the active part of the winding and of the end-winding body [12].

On the contrary, the use of numerical simulations can predict the temperature of a complex structure but the computational time for modeling is huge. These numerical simulations can be carried out by FEM or CFD. FEM-based simulations make it possible to compute the temperature accurately inside solid bodies. However, in order to take into account the effect of the fluid on the solid, convection heat transfer coefficients need to be applied at the boundaries between the solid zone and the moving fluid. These coefficients are provided by using analytical approaches or by some experimental tests. Using CFD simulation, the solid and the fluid regions can be modeled and the machine temperature is then analyzed with high accuracy. In fact, the exact evaluation of the temperature at different locations inside the machine is a very high CPU-time consuming task because of the complicity of the fluid velocity and of the surface properties of the machine [12]-[13]. In this paper, the CFD method is selected to analyze the temperature of the WRSM without cooling system.

B. Fluid Dynamic Model

The family of the Reynolds-Averaged Navier-Stokes (RANS) models is widely used in the field of turbulence for many industrial applications. In particular, RANS is the most widely used method for thermal analysis of electrical machines. Based on turbulent kinetic energy and dissipation rate or length scale transport equations, RANS models are commonly used for developing the turbulences arising from buoyancy, shear, or shocks.

For incompressible fluids, the density does not change with the pressure. The RANS equations can be described for fluid flow of an incompressible fluid by the following equations, see [14]:

$$\rho \frac{\partial U}{\partial t} + \rho(U.\nabla)U = -\nabla P + 2\nabla(\mu \nabla U) + f \qquad (3)$$
$$\nabla U = 0$$

where ρ is the density, U is the average velocity field, P is the pressure, μ is the dynamic viscosity and f is the volumetric force.

C. Simplified Structure

A simplified model of all the parts in the new corrected machine is created in 3D by ANSYS Maxwell. The complete model is required due to the lack of symmetry in the geometry of this machine. The thermal modeling of some parts such as winding, bearing is a challenging task. The bearing is thus not modeled in this study. In order to simplify the CFD model, some assumptions are made as follows, see [15]:

- The ambient temperature is constant.
- There is no influence of the temperature rise on the thermal property of materials.
- The lamination is modeled as an orthotropic composite material which has different thermal conductivities in different directions.
- Air is blown in and out perpendicular to the inlet and the outlet faces.
- Heat sources are uniformly distributed in the corresponding parts of the machine.

The winding is simplified as homogeneous winding thanks to the calculation of the equivalent conductivity. The winding has several different insulations such as wire insulation, slot insulation, wedges, etc. and they are modeled as an equivalent insulation system. In this paper, the winding insulation is simplified and it consists of only the wire insulation shown in Fig. 6.

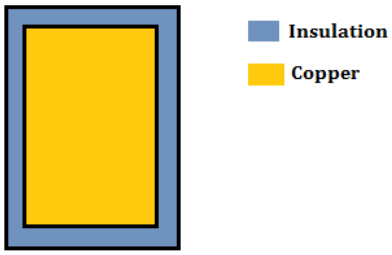

Fig.6. The copper and insulation components of a simplified winding.

The stator and the rotor are laminated in order to reduce eddy current losses. The laminations are separated by insulation which owns low thermal conductivity. Thus, the thermal conductivities of the stator and of the rotor in the axial direction is calculated as equivalent conductivity of the lamination and of the insulation [16]. Table V shows the thermal properties of the different materials used.

TABLE V
Thermal Properties of Materials

Material	Conductivity (W/mK)	Capacity (J/kgK)	Density (kg/m³)
Lamination	Radial (28) Axial (2)	420	7650
Copper	387	380	8960
Polyimide	0.26	1000	1449
Steel	16.27	502.48	8030
Aluminum	202.4	871	2719
Air	0.026	1000	1.22

D. Boundary Condition

Generally, the boundary conditions are necessary for the convergence of a CFD simulation. Regarding the inlet and the outlet regions, they are faces through which the air gets in and out from the simulation domain. The pressure inlet and the pressure outlet are used to define the flow boundary conditions at the inlet and at the outlet respectively, with zero Pa as the relative pressure for the natural convection [17]:

- Inlet: Pressure-inlet ($P = 0\ Pa$); $T_{amb} = 20°C$.
- Outlet: Pressure-outlet ($P = 0\ Pa$); $T_{amb} = 20°C$.
- Wall of moving fluid: Moving wall.
- The contact interfaces are considered as coupling surfaces.

E. Modeling Technique

The rotation of electrical machine has a direct effect on the fluid flow and the pressure distribution. There are two main techniques that can be used to simulate the machine rotation: moving reference frame (MRF) and sliding mesh (SM). For a steady state analysis, MRF technique is used and for a transient analysis, SM technique is used [18].

MRF technique is used to simulate the relative motion of the rotor and of the stator. The fluid region is split into two inner and outer regions by an interior surface. The inner fluid region surrounding the rotor part rotates at the machine speed. The outer fluid region is set to be stationary. The region where MRF is applied does not move physically, but rotation of all walls in the MRF region is taken into account to generate a constant grid flux. The grid flux is calculated based on the properties of the reference frame and therefore, the forces due to the rotation are introduced to the MRF region. This approach is suitable for a steady state analysis and it can solve most flow behavior like mass flow rate and pressure rise across rotating components [19].

F. Analysis Results

The k-ε realizable model with Enhanced Wall Treatment is used because of its robustness, and the solution methods are adjusted as second order [20]. The cell zone conditions govern the material, the heat generation and the rotational properties of the solid and of the fluid zones. Volumetric heat generation rates represent the iron and the copper losses. In natural convection, fluid motions are generated due to density differences caused by temperature differences. Therefore, air is considered as an incompressible ideal gas with specified operating conditions. To obtain these following results, 13 hours of CPU-time was needed using a PC-server with 16 processors (2.6GHz and 128GB).

The temperature distribution of the machine is shown in Fig. 7 and Fig. 8; the same temperature scales are used for both figures. The highest temperature in the machine is the temperature of the field winding (113.80°C). The surface temperature of the frame where the power converters are integrated is about 104.48°C. The error of the surface temperature of the frame between the CFD simulation and the analytical equation is about 8.05% with the same value of the losses analyzed by 3D electromagnetic simulations. However, it should be noticed that only natural convection is investigated in this study. The radiation should be taken into account at the surface of the machine frame for electrical machines without cooling system.

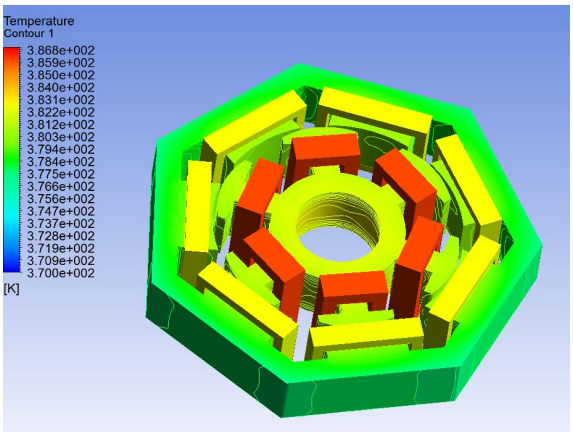

Fig. 7. Temperature distribution of the new corrected WRSM.

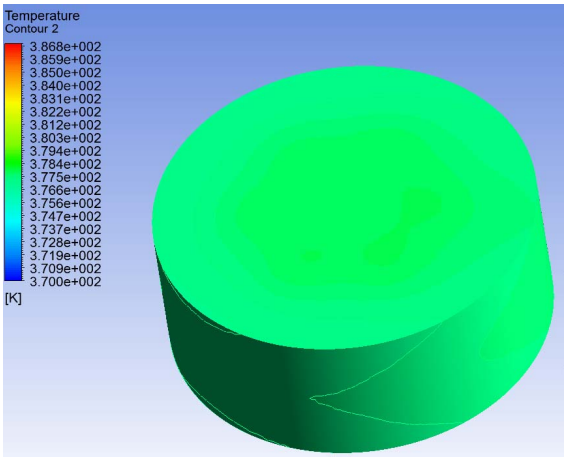

Fig. 8. Surface temperature of the new corrected machine frame.

V. Conclusion

The design optimization of a modular brushless wound rotor synchronous machine with 7 phases, 7 slots and 6 poles was investigated. 2D-numerical simulations were used inside the optimization code NOMAD in order to provide an optimal solution. Therefore, this optimal solution needs to be verified by using 3D electromagnetic and thermal analyses. The numerical validations show that using 3D electromagnetic simulations, the average torque is inferior to 5Nm. Hence, by increasing the length of the optimal machine, a new corrected WSRM is so-obtained. It can be observed that the iron losses obtained using 3D FEA are higher than in 2D. This is due to the high leakage flux in the end-winding of non-overlapping concentrated winding. By taking the values of losses analyzed by 3D FEM, the surface temperature of the new corrected machine calculated from (1) is different compared to the one analyzed by CFD simulation. It is important to note that the limit on the coil temperature was fixed to 105°C to guarantee a perfect functioning of the WSRM. Thus, in order to obtain that temperature value at the end of this entire design process, a limit of 85°C had to be fixed into the optimization problem. At the end, the coil temperature of the new corrected WSRM analyzed by CFD method is 113.48°C which is 8.48°C higher than the desired value. This should not be an issue, since we expect to have some dissipation by the shaft and the bearings of the machine. The results are very encouraging and shall be confirmed by an experimental test.

VI. REFERENCES

[1] Udai Shinpurkar, Henk Polinder, Jan A. Ferreira, "Modularity in Wind Turbine Generator Systems – Opportunities and Challenges", *Power Electronics and Applications*, 2016.

[2] Guang-Jin Li, Zi-Qiang Zhu, Martin P. Foster, Dave A. Stone, and Han-Lin Zhan, "Modular permanent-magnet machines with alternate teeth having tooth tips", *IEEE Trans. Industry Electronics*, vol. 62, no. 10, Oct. 2015.

[3] "Motor Technologies for Industry and Daily Life Edition", *Mitsubishi Electric Advance*, vol. 103, Sep. 2003.

[4] H.T. Le Luong, C. Hénaux, F. Messine, G. Bueno-Mariani, N. Voyer, S. Mollov, "Finite Element Analysis of a modular brushless wound rotor synchronous machine", *The 9th International Conference on Power Electronics, Machines and Drives*, Apr. 2018.

[5] Sébastien Le Digabel, "Blackbox optimization with the NOMAD software", GERAD and Ecole Polytechnique de Montréal (MAGI), CanmetEnergie, 2015.

[6] Dongsu Lee, Jong-Wook Kim, Cheol-Gyun Lee, and Sang-Yong Jung, "Variable mesh adaptive direct search algorithm applied for optimal design of electric machines based on FEA", *IEEE Trans. Magnetics*, vol. 47, no. 10, Oct. 2011.

[7] Myung-Ki Seo, Tae-Yong Lee, Jong-Wook Kim, Yong-Jae Kim, and Sang-Yong Jung, "Principal component optimization with mesh adaptive direct search for optimal design of IPMSM", *IEEE Trans. Magnetics*, vol. 53, no. 6, June 2017.

[8] Wei Tong, "Mechanical design of electric motors", CRC Press, Taylor & Francis Group, pp. 409-429.

[9] Huijuan Liu, Longya Xu, Mingzhu Shangguan, and W. N. Fu, "Finite element analysis of 1 MW high speed wound rotor synchronous machine", *IEEE Trans. Magnetics*, vol. 48, no. 11, Nov. 2012.

[10] ANSYS Maxwell 2D/3D user's guide.

[11] Juha Pyrhönen, Tapani Jokinen and Valéria Hrabovcova, "Design of rotating electrical machines", John Wiley & Sons, Ltd. ISBN: 978-0-470-69516-6, 2008.

[12] Han-Kyeol Yeo, Hyeon-Jeong Park, Jung-Moo Seo, Sang-Yong Jung, Jong-Suk Ro, and Hyun-Kyo Jung, "Electromagnetic and thermal analysis of a surface-mounted permanent-magnet motor with overhang structure", *IEEE Trans. Magnetics*, vol. 53, no. 6, June 2017.

[13] Roman Pechanek, Vladimir Kindl, Bohumil Skala, "Transient thermal analysis of small squirrel cage motor through coupled FEA", *Science Journal*, 2015.

[14] R. Pechanek, L. Bouzek, "Analyzing of two types water cooling electric motors using computational fluid dynamics", *15th International Power Electronics and Motion Control Conference*, 2012.

[15] Xinggang Fan, Ronghai Qu, Jian Li, Dawei Li, Bin Zhang and Cong Wang, "Ventilation and thermal improvement of radial forced air-cooled FSCW permanent magnet synchronous wind generators", *IEEE Trans. Industry Applications*, 2017.

[16] Mariia Polikarpova, "Liquid cooling solutions for rotating permanent magnet synchronous machines", Thesis for the degree of Doctor of Science at Lappeenranta University of Technology, Lappeenranta, Finland on the 21st of November, 2014.

[17] Shuye Ding, Hailing Li, "Investigation of characteristics of fluid flow pattern for air-cooled motor", *Industrial Electronics and Applications,* 2016.

[18] Peter H. Conner, Steve J. Pickering, Chris Gerada, Carol N. Eastwick, Chris Micallef, Chris Tighe, "Computational fluid dynamics modelling of an entire synchronous generator for improved thermal management", *IET Electric Power Applications*, 2012.

[19] P.H. Connor, S.J. Pickering, C. Gerada, C.N. Eastwick, C. Micallef, "CFD modelling of an entire synchronous generator for improved thermal management", *Power Electronics, Machines and Drives*, 2012.

[20] Unai San Andres, Gaizka Almandoz, Javier Poza, and Gaizka Ugalde, "Design of cooling systems using computational fluid dynamics and analytical thermal models", *IEEE Trans. Industrial Electronics*, vol. 61, no. 8, August 2014.

VII. BIOGRAPHIES

Huong Thao Le Luong received engineering degree in electrical engineering from ENSEEIHT – INP of Toulouse, France in 2013. From 2014, she was a research engineer in the Laboratory of Plasma and Energy Conversion, Toulouse, France. From 2015, she is a PhD Student in the Institut National Polytechnique de Toulouse, France. Her present work focuses on the optimal design of wound rotor synchronous machines.

Frederic Messine received his Master degree in 1993 and his Ph.D. in applied mathematics and computer science in September 1997. From 1998 to 2004 he was an associate professor in the University of Pau (France). From 2004 to 2013, he moved from the University of Pau to the high school ENSEEIHT-INPT of Toulouse in the IRIT Laboratory. In February 2006, he received his habilitation to supervise researches French diploma HdR. Since 2013, he does his research in the LAPLACE Laboratory of Toulouse and he became a full professor in September 2016. He does researches on deterministic global optimization, numerical optimal control, and topology optimization and on the applications of numerical optimization to solve inverse problems of electromechanical actuator designs.

Carole Henaux received the Dipl. Ing. Degree in Electrical Engineering from ENSEEIHT, Toulouse, France, in 1992 and the PHD degree from the Institut National Polytechnique de Toulouse in 1996. She is now a Lecturer with the Electrical Engineering department of INPT / ENSEEIHT. She teaches Electrical Machines modeling and is also the member of the Electrodynamics GREM3 research group of INPT-ENSEEIHT-LAPLACE, Toulouse. The group is of 9 permanent academics working in the fields of electromechanical energy conversion, with particular interest in novel techniques and design methodologies such as electroactive materials, composite magnetic materials, electroactive fluids, analytical field calculation and optimal design.

Guilherme Bueno Mariani received double engineering degree in electrical engineering in 2012 from the Grenoble-INP and from UNESP. In 2016 he received a Ph.D. degree in electrical engineering from the University of Grenoble Alpes. Since 2016, he is a researcher engineering at the Power Electronics Systems division at Mitsubishi Electric Research Centre Europe, Rennes, France. His present research interest is with the control, modeling and simulation of electrical machines.

Nicolas Voyer received engineering degree in digital communication from Telecom ParisTech in 1995. From 1997 to 2008, as research engineer in Mitsubishi Electric Information Technology Europe, Rennes, France, he contributed to the standardization of physical layer, signaling protocols and architecture of 3G and 4G cellular networks. From 2008, he is research manager in Power Electronics Systems division at Mitsubishi Electric Research Centre Europe, Rennes, France. His present research interest is with the control, modelling and simulation of power electronics systems, such as PV, railway and EV traction, HVDC. He is co-inventor of more than 80 patents.

Stefan V. Mollov received the Dipl.Eng. degree from the Technical University of Gabrovo, Gabrovo, Bulgaria, in 1995, and the Ph.D. degree from the University of Birmingham, Birmingham, U.K., in 2000. From 2000, he was a Lecturer with the University of Birmingham, where his research activities focused on power electronics applications in the field of autonomous systems, aerospace electrical systems, and renewable energy sources and storage. In 2005, he joined ADETEL Group, France, as a Power Electronics Expert, working on transport applications. In 2009, he joined THALES Avionics as a Power Supply Expert. Since 2013, he has been the Head of the Power Electronic Systems Division at the Mitsubishi Electric R&D Centre Europe, Rennes, France.